

PFC/JA-85-14

Progress in Tokamak Research at MIT

R. R. Parker, M. Greenwald, S. C. Luckhardt
E. S. Marmor, M. Porkolab, S. M. Wolfe

Plasma Fusion Center
Massachusetts Institute of Technology
Cambridge, MA 02139

April 1985

This work was supported by the U.S. Department of Energy Contract No. DE-AC02-78ET51013. Reproduction, translation, publication, use and disposal, in whole or in part by or for the United States government is permitted.

By acceptance of this article, the publisher and/or recipient acknowledges the U.S. Government's right to retain a non-exclusive, royalty-free license in and to any copyright covering this paper.

PROGRESS IN TOKAMAK RESEARCH AT MIT

R. R. Parker, M. Greenwald, S. C. Luckhardt, E. S. Marmor,
M. Porkolab, S. M. Wolfe

Plasma Fusion Center
Massachusetts Institute of Technology
Cambridge, Massachusetts 02139 USA

ABSTRACT

The major results and accomplishments of the MIT tokamak program are surveyed. These are considered to be 1) discovery of an ohmic-heating confinement law in which $\tau_E \propto \bar{n}aR^2$; 2) reduction of anomalous ion conduction to the neoclassical value by use of pellet fueling; 3) formulation of an empirical model for confinement of impurities in ohmically-heated tokamaks; 4) seminal experiments on current drive by lower hybrid waves and production of quasi-stationary driven current discharges with $n \sim 10^{20} \text{ m}^{-3}$; and 5) heating of electrons by Landau damping of lower hybrid waves with $\Delta T_e \sim 1 \text{ keV}$. The advance of $n_0 \tau_E$ is also traced from values of $\sim 10^{18} \text{ sec-m}^{-3}$ which were typical of tokamaks at the beginning of the Alcator program to values achieved on Alcator C in excess of $6 \times 10^{19} \text{ sec-m}^{-3}$, which is required for thermalized energy breakeven at higher temperature.

1. INTRODUCTION

For more than a decade, the Alcator experiments have pioneered the operation of tokamaks with strong toroidal magnetic fields. While the toroidal field itself has not played a role in the confinement of ohmically heated plasmas, the high current density $J_{\max} = 2B_T/\mu_0 R$ permitted by the high field and compact designs of Alcator A and C has provided strong ohmic heating power resulting in the capability to investigate plasma behavior over several orders of magnitude variation in plasma density ($5 \times 10^{18} \text{ m}^{-3} < n(0) < 2 \times 10^{21} \text{ m}^{-3}$). A set of machine and maximum plasma parameters produced in the ohmic heating regime in Alcator A and C is given in Table I.

TABLE I. MACHINE AND PLASMA PARAMETERS ASSOCIATED WITH THE ALCATOR A AND C TOKAMAKS ^a

Quantity	Alcator A	Alcator C
a (m)	0.10	0.10 - 0.17
R (m)	0.54	0.58 - 0.71
B _T (T)	9	13
I _p (kA)	300	800
n _{eo} (m ⁻³)	10 ²¹	2 × 10 ²¹
T _{eo} (keV)	2	3
T _{io} (keV)	1	1.6

^a The indicated variation in major radius corresponds to operation with a = 0.1 m. Except where explicitly stated in the text all experiments in Alcator C were carried out in the nominal geometry R = 0.64 m, a = 0.165 m. All other parameters represent maximum values for ohmically-heated plasmas.

The first MIT tokamak, Alcator A, began operation in 1972. Owing to severe impurity problems, the vacuum chamber was rebuilt in 1973 and plasma operation resumed in 1974. Several significant discoveries and experiments then occurred in rapid succession including 1) discovery of a "slide-away" regime characterized by high values of the drift velocity $J_{\parallel}/(ne) > (KT_e/m_i)^{1/2}$; 2) observation of a regime in which the energy confinement time τ_E increased linearly with average density \bar{n} ; 3) development of methods of discharge control and vacuum chamber preparation leading to the first reliable operation of tokamaks with $Z_{\text{eff}} \approx 1$; and 4) initial RF heating experiments using waveguide coupling of lower hybrid waves [1]. Operation at high densities ($> 10^{20} \text{ m}^{-3}$) resulted in the first achievement of the Lawson parameter $n_0 \tau_E$ of $1 \times 10^{19} \text{ sec-m}^{-3}$ in 1975 [2, 3]. Optimization of the high density and high field plasmas produced in Alcator A led to further increase of $n_0 \tau_E$ to the value $3 \times 10^{19} \text{ sec-m}^{-3}$ in 1978 [4].

Alcator C was designed in 1976 and began operation in 1978. The primary objective was to extend the performance of the high density plasma regimes explored first in Alcator A, and thereby achieve a Lawson parameter approaching $10^{20} \text{ sec-m}^{-3}$. However, early confinement measurements showed an unexpected saturation in τ_E vs. \bar{n} due to enhanced ion conduction with respect to the neoclassical value. This was in contrast with results achieved on Alcator A in which the ion conduction was found to be in agreement with neoclassical transport. In experiments designed to elucidate the dependence of confinement on geometry, it was found that in the regime in which $\tau_E \propto \bar{n}$, τ_E varied as the cube of the size rather than the square as had been widely believed [5]. Further, the experiments revealed a stronger dependence on R than a, and

these observations ultimately led to the announcement of the neo-Alcator scaling law $\tau_E \propto \bar{n} R^2 a$ in 1982 [6, 7]. Shortly thereafter, it was discovered that by changing the method of fueling from gas-puffing to pellets, the anomalous ion conduction could be suppressed; using this technique plasmas were produced in 1983 with $n_0 \tau_E$ in excess of that required for breakeven at higher temperature [8].

In addition to data on energy confinement and transport, the Alcator A and C tokamaks have been used to collect an extensive data set on the behavior of impurities in ohmically-heated plasmas. Using the laser blow-off technique, trace amounts of impurities have been injected and the transport measured by spectroscopic means. In all cases which have been studied, the impurity confinement time τ_I has been finite and accumulation does not occur. The results can be summarized conveniently by the empirical scaling law $\tau_I \propto a m_{bg} q^{-1}$ where m_{bg} is the mass of the background gas and q is the safety factor [9]. A dependence on Z_{eff} has also been observed.

The MIT tokamaks have also made important contributions to the development of lower hybrid heating and current drive. These experiments were begun on Alcator A using a single waveguide coupler to deliver 100 kW of power at 2.45 GHz [1, 10]. An important milestone was the demonstration in 1980 of current drive using lower hybrid waves at 800 MHz on the Versator II tokamak [11], a relatively small-scale, low field research tokamak. Versator I, the first U.S. small-scale research tokamak, was built in 1973 and provided useful information concerning the control of impurities in tokamaks by discharge cleaning. The lower hybrid program was continued on Alcator C, and continues to provide a focus for the

Alcator C program. A maximum of just over 1 MW of power at 4.6 GHz has been coupled to the plasma using up to three 4×4 waveguide arrays. These experiments have demonstrated flat-top RF current drive at densities approaching 10^{20} m^{-3} [12], and in the electron heating Landau-damping mode, electron heating of about 1 keV [13].

2. CONFINEMENT IN OHMICALLY-HEATED ALCATOR A AND C PLASMAS

2.0. The Slide-Away Regime in Alcator A

The initial operation of Alcator A was characterized by clean ($Z_{\text{eff}} \approx 1$) discharges which allowed variation of plasma density over nearly two orders of magnitude, $5 \times 10^{18} \text{ m}^{-3} < n < 2 \times 10^{20} \text{ m}^{-3}$. By operating with low plasma density and moderately high field, high values of the streaming parameter $\xi = (J_{\parallel}/ne)/(KT_e/m_i)^{1/2}$ were obtained and this resulted in discovery of the slide-away regime [1, 14]. The characteristics of the regime are: 1) $\eta(0)/\eta_{c1} < 1$ where $\eta(0)$ is the on-axis resistivity and η_{c1} is the Spitzer-Härm value at the measured electron temperature; 2) anomalous ion heating due to turbulence with $\omega \gtrsim \omega_{pi}$; and 3) non-Maxwellian x-ray spectra with tails extending in energy for $E \gg KT_e$. The onset of the slide-away mode occurred for $\xi > \xi_c$ where $\xi_c \approx 0.3$ in H_2 , 0.2 in D_2 and 0.1 in He. The presence of the anomalous ion heating and the absence of hard x-radiation distinguished this mode from the conventional run-away discharge commonly observed in other tokamaks at the time.

2.1. Energy Confinement

Energy confinement was investigated on the Alcator A tokamak over a wide range of plasma parameters. The most significant and unexpected result of these studies was the observation [1, 2] that the global energy

confinement time τ_E increased approximately linearly with line averaged density, as shown in Fig.1. Neoclassical theory predicted that energy confinement should be limited by ion thermal conduction losses and τ_E should scale inversely as the density, contrary to the experimental result. Analysis [4] of the power balance in the central half of the plasma column indicated a significant anomaly in the electron thermal diffusivity χ_e , which scaled as $\chi_e \propto 1/\bar{n}_e$. At $\bar{n}_e = 10^{20} \text{ m}^{-3}$, $\chi_e \approx 200$ times the neoclassical value. At the highest values of \bar{n}_e , power flow in the center of the plasma was found to be dominated by ion thermal conduction consistent with neoclassical predictions and $\chi_e < 10 \chi_e^{\text{Neo}}$. No saturation was observed in global confinement, however, and the value of the Lawson parameter $n_0 \tau_E$ increased quadratically with increasing \bar{n}_e up to a maximum of $3 \times 10^{20} \text{ m}^{-3} \text{ sec}$ at $\bar{n}_e \approx 7 \times 10^{20} \text{ m}^{-3}$ [2, 3, 4].

Studies of energy confinement in high density, high field discharges were continued on the larger Alcator C tokamak. Initial experiments used gas fueling to increase the density, as on Alcator A. Typical scaling results in these plasmas are shown by the solid points in Fig.2. An approximately linear dependence of τ_E on density was found for $\bar{n}_e < 2.5 \times 10^{20} \text{ m}^{-3}$, but at higher density a partial saturation occurred. Departure from a linear scaling at high density was theoretically predicted due to neoclassical ion thermal conduction, and this effect had been previously observed [4, 15]. However, in the present case the saturation appeared at significantly lower \bar{n}_e and τ_E values than predicted by theory. An anomaly factor of roughly 3 relative to the Chang-Hinton neoclassical thermal diffusivity [16] is required to account for the data on the basis of ion losses. Experiments on other tokamaks [17, 18, 19] also suggested the existence of anomalously high ion losses.

Analysis of experiments on Alcator C carried out at relatively low density ($\bar{n}_e < 3 \times 10^{20} \text{ m}^{-3}$) supported the interpretation that anomalous ion conduction was present in these discharges. At higher density the equilibration between central electron and ion temperatures was too close to permit a meaningful calculation of the ion power balance. Scaling studies [6, 7] indicated that the anomaly increased with plasma current as shown in Fig.3. The maximum inferred value of χ_1 in this data set was approximately $1 \text{ m}^2\text{sec}^{-1}$, corresponding to a ratio $\chi_1/\chi_1^{\text{Neo}}$ of 7 with respect to the Hinton-Hazletine coefficient [20] or approximately 4 with respect to the Chang-Hinton formulation.

While the mechanism for the confinement saturation was not known, several observations focused our attention on fueling and particle transport. The saturation began near the density at which the plasma became completely opaque to charge-exchange neutrals (i.e., the neutral mean free path was less than the density scale length everywhere in plasma). At higher densities, strong gas puffing was required and τ_p^* , the global particle confinement time, dropped. Density profiles were broad (peak to average ratios of 1.2 - 1.4) for virtually all operating conditions. In order to investigate these issues an alternative to gas fueling was needed. A pellet injector was built (based on ORNL designs) and a series of pellet fueling experiments was begun [8].

Injection of high-speed pellets provided a means for directly fueling the core of the tokamak discharge [21, 22]. The injector used on Alcator C produced 1 - 4 pellets of hydrogen or deuterium and accelerated them pneumatically to velocities near 1 km/sec. The pellets, each about 1 mm in size, contained 7×10^{19} atoms which corresponded to $\Delta\langle n_e \rangle = 2 \times 10^{20} \text{ m}^{-3}$.

In the Alcator C plasmas, these pellets lasted for 100 - 150 μ sec and deposited fuel over a broad area centered near $r = a/2$. The density profiles that were produced were initially hollow but filled in in less than 500 μ sec. After this initial transient, the profiles became peaked, retaining a peak to average value of 2 as the density slowly decayed in 100 - 150 msec. The electron and ion temperatures dropped as cold fuel from the pellet diluted the hot plasma. The plasma temperature recovered more quickly than the density, reheating in 15 - 40 msec, the longer times corresponding to higher densities.

The plasma energy content, evaluated by integrating density and temperature profiles rose after injection and peaked as the temperature recovered. This observation was confirmed by a rise in β_p obtained from magnetic measurements. Values of β_p as high as 0.5 were observed at $I_p = 780$ kA, corresponding to a plasma energy of 80 kJ. For these plasmas the average pressure was .16 MPa with pressures above .8 MPa on axis. Confinement times were evaluated in the quasi-static portion of the discharge, 30 - 50 msec after injection when the temperature had recovered and contributions from transients were relatively small. Results of these calculations are shown by the open points in Fig.2 where the energy confinement time is plotted vs line-averaged density. Confinement times of the pellet fueled shots did not show the saturation at $2.5 \times 10^{20} \text{ m}^{-3}$ and were as much as 70% higher than the gas fueled shots at the highest density. The figure also compares the experimental data with results of a computer simulation in which transport was modeled with $\chi_e \propto 1/n_e$ and $\chi_i = 1 \times \text{neoclassical}$. The confinement parameter $n_0 \tau_E$ is plotted for these shots in Fig.4. Due to improved confinement and peaked density profiles the difference between gas puffing and pellet fueling became even clearer

with several of the shots exceeding the Lawson $n\tau$ criterion for thermalized breakeven at higher temperatures [23].

As discussed above, studies of the saturated confinement regime led to the conclusion that the additional energy losses that were observed were through the ion channel. A direct comparison with pellet discharges was made by running the ONETWO code [24] in analysis mode, assuming ion conductivity of the neoclassical form, and calculating the anomaly factor. Inputs for this calculation were the measured electron density and temperature profiles, plasma current, Z_{eff} , and the total neutron rate. Results are shown in Fig.5, where the neoclassical multiplier is plotted against time, and shows a clear decrease in ion transport after injection. This calculation showed no change in electron thermal conductivity. The result is subject to large errors because T_e and T_i are very close, but the qualitative behavior is quite reproducible.

Use of limiters smaller than the nominal 0.165 m in Alcator C permitted direct investigation of the scaling of energy confinement with plasma size and aspect ratio. Both major and minor radius were varied in a series of experiments [5] which spanned aspect ratios $3.9 < A < 7.05$. In all cases, τ_E exhibited a linear dependence on density at low to moderate \bar{n} , followed by a slower rise or saturation similar to that in Fig.2. Comparison of the values of τ_E in the linear, electron dominated regime revealed a strong dependence on major radius and relatively weak scaling with minor radius. The Alcator C data, together with the earlier result from Alcator A, were well fit by a regression

$$\tau_E^{\text{Alc-C}}/\bar{n}_e = 1.15 \times 10^{-21} R^{2.3} a^{0.8}$$

which agreed well with data from other ohmically heated tokamaks. Regression analysis applied to results from twelve facilities led to the "Neo-Alcator Scaling" [5, 7]

$$\tau_E^{\text{NeoAlc}}/\bar{n}_e = 1.92 \times 10^{-21} R^{2.04} a^{1.04}.$$

The fit to this regression parameter is shown in Fig.6; the points representing the large tokamaks TFTR and JET were obtained subsequently and were not included in the analysis.

Similar scalings had been proposed previously, based on extensive statistical analyses of the tokamak database [25], and on experiments in which the minor radius was varied [26]. Moreover, the result that τ_E should vary with approximately the third power of the linear dimensions, rather than the second, may be obtained from rather general theoretical considerations for a large class of transport mechanisms [27]. The Alcator C results represented the first direct experimental evidence for such a dependence on major radius of the energy confinement time. The striking agreement of data from the new large devices [28, 29] with the neo-Alcator prediction is a strong confirmation of this result.

2.2. Impurity Transport

Since impurities play an important role in determining the characteristics of all tokamak fusion plasmas, the study of impurity transport has formed the basis of a large set of experiments [9, 30] on both the Alcator A and C devices. Utilizing the laser blow-off technique [31], trace amounts of Al, Si, Ti, Fe, Mo and W have been introduced into the plasma. Subsequent emissions from the various charge states have been monitored

with a variety of UV and x-ray instruments. A parametric study of injections has been performed over the full range of Alcator A and C operating conditions.

A detailed look at specific Si emission lines during a sequence of similar deuterium discharges on Alcator C ($B_T = 6$ T, $I = 385$ kA, $\bar{n}_e = 3.6 \times 10^{20} \text{ m}^{-3}$, $T_e = 1100$ eV, and $q_L = 3.13$) is provided in Fig.7, where the normalized chordal brightness of sodium-, beryllium-, helium-, and hydrogen-like silicon, as well as the central-chord soft-X-ray brightness, are shown after the injection. The peaks of the emissions occurred sequentially in time as the silicon is ionized and transported to the plasma center. Each signal then decayed to its pre-injection level, indicating that the silicon left the plasma on a time scale shorter than the discharge length, with little or no re-cycling.

These types of observations have been compared to the predictions of a 1-D impurity transport code [32] in an effort to understand the impurity transport mechanisms in Alcator C. The predictions for the plasma conditions of Fig.7, when the impurity flux is taken to have the neoclassical form [33] are in qualitative disagreement with the data. A purely diffusive model predicts an exponential decay for the emissions from the centrally located ionization states shortly after the peaks. The falling signal of Si^{12+} in Fig.1 is well described by an exponential and yields a decay time of 19 ms. This characteristic time is interpreted as the global particle confinement time for non-re-cycling injected trace impurities.

The dependence of impurity confinement time on limiter safety factor is exhibited in Fig.8, where the impurity confinement times for aluminium, silicon and titanium are plotted against $1/q_L$ for hydrogen, deuterium and

helium discharges. In addition, Fig.8 includes data from a wide range of toroidal fields ($3 \text{ T} < B_t < 12 \text{ T}$). q_L^{-1} appears to be the relevant parameter since the confinement times decrease with increasing toroidal field. The slopes of the three lines are in the ratio 4:2:1, indicating a linear dependence on the mass of the background ion. τ_I is independent of impurity species, and experiments with Mo and W have shown that this is true for differing Z_I/m_I as well.

Summarizing these scalings the impurity confinement time may be described as

$$\tau_I(\text{ms}) = \frac{1.7 \times 10^2 a_L m_{bg}}{q_L} \frac{Z_{eff}}{Z_{bg}}$$

with a_L in m, m_{bg} in amu, and where Z_{bg} is the charge of the background ion. For the centrally located ionization states, τ_I is independent of the charge and mass of the impurity, and the electron density (provided there is little or no MHD ($m > 2$) activity). The dependence on Z_{eff} should not be interpreted too literally, and there may be some dependence on major radius (R^α , $0 < \alpha < 1$). It is, however, well established empirically from these results that τ_I is approximately proportional to $a_L m_{bg} q_L^{-1}$.

While the τ_I 's and τ_E 's observed on the Alcator devices are of similar magnitude, their scalings with plasma parameters are markedly different. In particular, the absence of τ_I dependence on n_e is striking, and its scaling with major radius is much weaker than the R^2 dependence seen for the energy confinement.

3. RF HEATING AND CURRENT DRIVE EXPERIMENTS

3.1. Lower Hybrid Heating Experiments on Alcators A and C

Lower hybrid heating experiments have had a long history at MIT [10]. The first heating experiment was carried out on the Alcator A device in 1975 [1]. A single waveguide was used to inject up to 70kW of RF power at 2.45 GHz. An apparent ion heating of $\Delta T_i \sim 100\text{eV}$, as well as ion tail formation, was observed, even though the lower hybrid layer was not present in the plasma column. These experiments were repeated in 1980-1981 with a phased double waveguide array, with similar results [34]. The heating observed was independent of waveguide phasing. Strong parametric instability activity, which was observed on probes located in the scrape-off layer, may have been partially responsible for the observed ion tail activity. In addition, scattering of the waves by low-frequency turbulence may have produced partial wave penetration and accessibility in the relatively small [$a = 0.10\text{ m}$] plasma column [35].

High power ($P \lesssim 1\text{ MW}$) lower hybrid experiments at $f = 4.6\text{ GHz}$ were carried out in the Alcator C tokamak in recent years (1982 - 1985) [12, 13, 36-38]. In these experiments up to three phased waveguide arrays, each consisting of 4×4 elements, were used to inject the RF power. In some cases the maximum transmitted power density attained values as high as 90 MW/m^2 in the waveguide and its internal ceramic window.

Phasing the adjacent waveguides by 180° , significant electron and ion heating was observed at line average densities of $\bar{n}_e \approx 1.5 \times 10^{20}\text{ m}^{-3}$ in both deuterium and hydrogen plasmas. Upon injecting 850 kW of power, the electron temperature rose from 2.0 keV to 3.0 keV, and the ion

temperature rose from 1.0 keV to 1.8 keV [13, 37, 38]. Typical heating results are reproduced in Figs 9a and 9b. In this regime $\omega \gtrsim 2\omega_{\text{LH}}(0)$ (where $\omega_{\text{LH}}(0)$ is the lower hybrid frequency) and hence the heating mechanism is by way of electron Landau absorption, with subsequent collisional equilibration with ions. Heating efficiencies as high as 80% were predicted by transport and ray-tracing code simulations of these experiments [13]. At higher densities ion tails were observed, but no bulk ion heating. It was shown that the ion tails were a by-product of parametric decay instabilities near the plasma surface [39]. For the first time, both the parametric decay wave, and the injected pump wave spectrum were measured by collective scattering using a CO₂ laser beam [39, 40]. Reasonable agreement with the theoretically predicted wave spectrum was found in these experiments. Excessive collisional damping is believed to be the main mechanism which prevented pump wave penetration in the higher density ($\bar{n}_e > 2 \times 10^{20} \text{ m}^{-3}$) bulk ion heating regime.

3.2. Lower Hybrid Current Drive Experiments on Alcator C

RF current drive and ramping experiments were carried out at densities $\bar{n}_e = 1 \times 10^{19} - 1 \times 10^{20} \text{ m}^{-3}$. The relative phases of the waveguides were set at $\Delta\phi = 67.5^\circ - 135^\circ$, with a typical phasing of 90° . Flat-top toroidal currents up to 230 kA were generated by injecting up to 1.0 MW of RF power, with the inductive drive terminated. Pulse durations were up to 0.4 sec, well in excess of the typical $\sim 100 - 150$ msec L/R times. The efficiencies were determined by varying the RF power, density, current, and toroidal magnetic field. As shown in Fig.10, the current drive efficiency at $B = 10\text{T}$ was $\eta = \bar{n}_e (10^{20} \text{ m}^{-3}) I(\text{MA})/P(\text{MW}) = 0.19$, and at $B = 8\text{T}$ $\eta = 0.13$ was achieved [12, 36, 38]. Radial measurements of the high energy x-ray spectra indicated that the high energy electrons peaked on

axis, in contradiction with ray-tracing code calculations which predict RF power deposition off-axis. By increasing the power above that needed for flat-topping the current, ramping was observed. Because of the high densities, ($\bar{n}_e \gtrsim 1 \times 10^{19} \text{ m}^{-3}$) at most 10% of the RF power only was converted into poloidal field energy. Transformer recharging experiments were also carried out, and it was shown that, given a long enough RF pulse, the Alcator C transformer could have been recharged in two seconds. Most recently, a series of energy confinement scaling experiments were begun in the presence of purely RF driven currents. The energy confinement time is close to the ohmic value at $\bar{n} \sim 2-3 \times 10^{19} \text{ m}^{-3}$, but exhibits a density-independent scaling.

3.3. ICRF Experiments on Alcator C

Using a 500 kW RF system at $f = 180 \text{ MHz}$, fast wave ion cyclotron heating experiments were carried out at $B = 12\text{T}$, [41] which corresponds to the proton minority regime in a deuterium background plasma. With approximately 3% minority ion concentration, upon injection of 400 kW RF power the bulk deuterium temperature increased by $\Delta T_1 \sim 600 \text{ eV}$ at a maximum line average density of $\bar{n}_e = 1.9 \times 10^{20} \text{ m}^{-3}$ [41]. No significant change in the electron temperature was observed. These experiments will be continued in the near future, including both fast wave and Bernstein wave launchers.

3.4. Lower-Hybrid Current Drive on the Versator II Tokamak

The Versator II tokamak is a small research tokamak at MIT ($R_0 = 0.40 \text{ m}$, $a = 0.13 \text{ m}$, $B_t = 1.5 \text{ T}$) on which experiments have been performed since 1979 on the generation of toroidal currents using traveling lower-hybrid waves [11]. These were the first tokamak experiments which unambiguously

identified lower-hybrid RF current drive. Experiments were carried out with up to 100 kW of RF power at a frequency of 800 MHz, and more recently with $f = 2.45$ GHz with RF pulse length comparable to or longer than the plasma L/R time. In all experiments phased arrays of either four or six waveguides were employed to couple RF power into the plasma.

By launching traveling waves in the electron ohmic drift direction, ($\Delta\phi > 0$), the total toroidal current (RF generated plus inductively driven) increased substantially, while the single turn loop voltage was reduced to near zero (or even negative) values. As shown in Fig.11a, the incremental current, ΔI , was found to be strongly dependent on the relative waveguide phasing, $\Delta\phi$, with a maximum at $\Delta\phi = +90^\circ$, while the transmission coefficient, T , was symmetrical about $\Delta\phi = 0$ (Fig.11b). An extensive set of experiments demonstrated that these effects were not produced by inductive electric fields, or by electron heating, and RF currents greater than 10 kA were generated [11]. Furthermore, a current drive density limit was identified; when the density was increased above $\bar{n} = 6 \times 10^{18} \text{ m}^{-3}$, corresponding to a parameter $\omega/\omega_{LH}(0) \approx 1.5$, there was a significant reduction in the current drive efficiency (Fig.11c). The most recent experiments on Versator II have shown that the density limit can be increased to above $\bar{n}_e \gtrsim 10^{19} \text{ m}^{-3}$ (i.e., $\omega_{pe}^2/\omega_{ce}^2 \gtrsim 1$) by raising the frequency to $f = 2.45$ GHz [42].

A significant feature of the 800 MHz experiments was the appearance of the anisotropic electron tail drive electron plasma wave instability [43]. It was shown that this mode activity could be suppressed by the application of sufficient electron cyclotron heating power ($f = 35$ GHz, $P \gtrsim 15$ kW,

NRL gyrotron) [43]. Concomitant improvement in the global particle confinement time was also observed in these experiments [44].

4. CONCLUSIONS

The tokamak program at MIT has made many important contributions to the scientific understanding and development of the tokamak concept. The high current density and compact designs of Alcator A and C, together with development of reliable methods of impurity control have permitted operation over extraordinarily wide ranges of plasma parameters. In the ohmic-heating regime, the major results have been associated with elucidation of the dependence of confinement on density and geometry, leading to the Neo-Alcator confinement law $\tau_E \propto \bar{n}R^2a$. This result has been verified by the ohmically-heated performance of JET and TFTR. Exploiting the dependence on density, the Alcator tokamaks have led the way in improving $n_0\tau_E$ from $\sim 1 \times 10^{18} \text{ sec-m}^{-3}$, characteristic of tokamaks in the early 1970's, to values in excess of that required for breakeven (at higher temperature), $n_0\tau_E > 6 \times 10^{19} \text{ sec-m}^{-3}$. Lower hybrid heating and current drive has also been an area of major contribution. The first U.S. demonstration of current drive was carried out on the Versator II device, and using the unique high-field capabilities of Alcator C, stationary driven-current plasmas have been produced at densities approaching 10^{20} m^{-3} , with efficiency within a factor of 2 of that predicted by theory. Finally, efficient heating of Alcator C plasmas by lower hybrid power has also been obtained, resulting in electron temperature increases of 1 keV at densities in excess of 10^{20} m^{-3} . The lower hybrid experiments and also ICRF heating studies are continuing and provide a current focus of the Alcator C program.

ACKNOWLEDGEMENTS

This work supported by U.S. Department of Energy contract number
DE-AC02-78ET51013.

REFERENCES

- [1] BOXMAN, G. J., COPPI, B., deKOCK, L. C. J. M., MEDDENS, B. J. H., OOMENS, A. A. M., et al., in Seventh European Conference on Controlled Fusion and Plasma Physics (Proc. 7th Eur. Conf. Lausanne, 1975) Vol. 2, EPS, Petit-Lancy, Switzerland (1975) 14.
- [2] APGAR, E., COPPI, B., GONDHALEKAR, A., HELAVA, H., KOMM, D., et al., in Plasma Physics and Controlled Nuclear Fusion Research 1976 (Proc. 6th Int. Conf. Berchtesgaden, 1976) Vol. 1, IAEA, Vienna (1977) 247.
- [3] GAUDREAU, M., et al., Phys. Rev. Lett. 39 (1977) 1299.
- [4] GONDHALEKAR, A., GRANETZ, R., GWINN, D., HUTCHINSON, I., KUSSE, B., et al., in Plasma Physics and Controlled Nuclear Fusion Research 1978 (Proc. 7th Int. Conf. Innsbruck, 1978) Vol. 1, IAEA, Vienna (1979) 199.
- [5] BLACKWELL, B., FIORE, C. L., GANDY, R., GONDHALEKAR, A., GRANETZ, R. S., et al., in Plasma Physics and Controlled Nuclear Fusion Research 1982 (Proc. 9th Int. Conf. Baltimore, 1982) Vol. 2, IAEA, Vienna (1983) 27.
- [6] PARKER, R. R., Energy Confinement in Alcator C: Neo-Alcator Scaling, Bull. Am. Phys. Soc. 27 (1982) 986. (Abstract)
- [7] ALCATOR GROUP, Alcator C Status and Program Plan, MIT Plasma Fusion Center Report PFC/IR-82-3 (December 1982).
- [8] GREENWALD, M., GWINN, D., MILORA, S., PARKER, J., PARKER, R., et al., Phys. Rev. Lett. 53 (1984) 352.
- [9] MARMAR, E. S., RICE, J. E., TERRY, J. L., SEGUIN, F. H., Nucl. Fusion 22 (1982) 1567.
- [10] PARKER, R. R., RLE-MIT Quarterly Progress Report 102, Cambridge, MA, (July 1971).
- [11] LUCKHARDT, S., PORKOLAB, M., KNOWLTON, S. S., CHEN, K-I., FISCHER, A. S., Phys. Rev. Lett. 48 (1982) 152.
- [12] PORKOLAB, M., SCHUSS, J. J., LLOYD, B., TAKASE, Y., TEXTER, S., et al., Phys. Rev. Lett. 53 (1984) 450.
- [13] PORKOLAB, M., LLOYD, B., TAKASE, Y., BONOLI, P., FIORE, C., et al., Phys. Rev. Lett. 53 (1984) 1229.
- [14] OOMENS, A. A., ORNSTEIN, L. Th. M., PARKER, R. R., SCHÜLLER, F. C., TAYLOR, R. J., Phys. Rev. Lett. 36 (1976) 255.
- [15] MURAKAMI, M., BURRELL, K. H., JERNIGAN, T. C., AMANO, T., BATES, S. C., et al., in Plasma Physics and Controlled Nuclear Fusion Research 1978 (Proc. 7th Int. Conf. Innsbruck, 1978) Vol. 1, IAEA, Vienna (1979) 269.

- [16] CHANG, C. S., HINTON, F. L., *Phys. Fluids* 25 (1982) 1493.
- [17] PLT GROUP, in *Plasma Physics and Controlled Nuclear Fusion Research 1978* (Proc. 7th Int. Conf. Innsbruck, 1978) Vol. 1, IAEA, Vienna (1979) 167.
- [18] EQUIPE TOKAMAK FONTENAY-AUX-ROSES, *Nucl. Fusion* 18 (1978) 1271.
- [19] EJIMA, S., PETRIE, T. W., RIVIERE, A. C., ANGEL, T. R., ARMENTROUT, C. J., et al., *Scaling of Energy Confinement with Minor Radius, Current and Density in Doublet III Ohmically Heated Plasmas*, General Atomic Company Report GA-A16497 (March 1982).
- [20] HINTON, F. L., HAZLETINE, R. D., *Rev. Mod. Phys.* 48 (1976) 239.
- [21] SPITZER, L., GROVE, D., JOHNSON, W., TONKS, L., WESTENDORP, W., U.S. Atomic Energy Commission, NYO-6047 (1954).
- [22] MILORA, S. L., *Journal of Fusion Energy* 1 (1981) 15.
- [23] LAWSON, J. D., *Proc. Phys. Soc. London, Sect. B* 70 (1957) 6.
- [24] PFEIFFER, W. W., DAVIDSON, R. H., MILLER, R. L., WALTZ, R. E., ONETWO: A Computer Code for Modeling Plasma Transport in Tokamaks, General Atomic Company Report GA-A16178 (1980).
- [25] PFEIFFER, W., WALTZ, R. E., *Nucl. Fusion* 19 (1979) 51.
- [26] LEONOV, V. M., MEREZHKIN, V. G., MUKHOVATOV, V. S., SANNIKOV, V. V., TILININ, G. N., in *Plasma Physics and Controlled Nuclear Fusion Research 1980* (Proc. 8th Int. Conf. Brussels, 1980) Vol. 1, IAEA, Vienna (1981) 394.
- [27] CONNOR, J. W., TAYLOR, J. B., *Nucl. Fusion* 17 (1977) 1047.
- [28] GOLDSTON, R., *Plasma Physics and Controlled Nuclear Fusion* 26 (1984) 87.
- [29] REBUT, P. H., BARTLETT, D. V., BAUMEL, G., BEHRINGER, K., BEHRISCH, R., et al., in *Plasma Physics and Controlled Nuclear Fusion Research 1984* (Proc. 10th Int. Conf. London, 1984) IAEA, Vienna (1985).
- [30] MARMAR, E. S., RICE, J. E., ALLEN, S. L., *Phys. Rev. Lett.* 45 (1980) 2025.
- [31] MARMAR, E., CECCHI, J., COHEN, S., *Rev. Sci. Instrum.* 46 (1975) 1149.
- [32] MARMAR, E. S., *Transport of Injected Impurities in the ATC Tokamak*, Ph.D. Thesis, Princeton University (1976) (unpublished).
- [33] HAWRYLUK, R. J., SUCKEWER, S., HIRSHMAN, S. P., *Nucl. Fusion* 19 (1979) 607.
- [34] SCHUSS, J. J., PORKOLAB, M., TAKASE, Y., COPE, D., FAIRFAX, S., et al., *Nucl. Fusion* 21 (1981) 427.

- [35] BONOLI, P. T., OTT, E., Phys. Fluids 25 (1982) 359.
- [36] PORKOLAB, M., SCHUSS, J. J., TAKASE, Y., TEXTER, S., BLACKWELL, B., et al., in Plasma Physics and Controlled Nuclear Fusion Research 1982 (Proc. 9th Int. Conf. Baltimore, 1982) Vol. 1, IAEA, Vienna (1983) 227.
- [37] PORKOLAB, M., LLOYD, B., SCHUSS, J. J., TAKASE, Y., TEXTER, S., et al., in Europhysics Conference Abstracts (Proc. 11th Eur. Conf. Aachen, 1983) Vol. 7D, Part 1, EPS, Petit-Lancy, Switzerland (1983) 269.
- [38] PORKOLAB, M., LLOYD, B., SCHUSS, J. J., TAKASE, Y., TEXTER, S., et al., in Heating in Toroidal Plasmas (Proc. 4th Int. Symp. Rome, 1984) Vol. 1, International School of Plasma Physics, Varenna (1984) 529.
- [39] TAKASE, Y., WATTERSON, R. L., PORKOLAB, M., FIORE, C. L., SLUSHER, R. E., et al., Phys. Rev. Lett. 53 (1984) 274.
- [40] WATTERSON, R., TAKASE, Y., BONOLI, P. T., PORKOLAB, M., Spectrum and Propagation of Lower Hybrid Waves in a Tokamak Plasma, MIT Plasma Fusion Center Report PFC/JA-84-6 (March 1984). To be published in Phys. Fluids.
- [41] PORKOLAB, M., BLACKWELL, B., BONOLI, P., GRIFFIN, D., KNOWLTON, S., et al., in Plasma Physics and Controlled Nuclear Fusion Research 1984 (Proc. 10th Int. Conf. London, 1984) Vol. 1, IAEA, Vienna (1985) 463.
- [42] MAYBERRY, M., LUCKHARDT, S. C., PORKOLAB, M., CHEN, K-I., GRIFFIN, D., et al., The Versator II 2.45 GHz Lower-Hybrid Current Drive Experiment, Bull. Am. Phys. Soc. 29 (1984) 1248. (Abstract)
- [43] LUCKHARDT, S. C., BEKEFI, G., BONOLI, P. I., CHEN, K-I., COPPI, B., et al., in Heating in Toroidal Plasmas, (Proc. 3rd Joint Varenna-Grenoble Int. Symp. Grenoble) Vol. 2, International School of Plasma Physics, Varenna (1982) 529.
- [44] LUCKHARDT, S., CHEN, K-I., MAYBERRY, M. J., PORKOLAB, M., TERUMICHI, Y., et al., Particle Confinement and the Anomalous Doppler Instability during Combined Inductive and Lower-Hybrid Current Drive, MIT Plasma Fusion Center Report PFC/JA-84-42 (December 1984).

FIGURE CAPTIONS

- FIG.1 Energy confinement time vs line-averaged density for Alcator A. The neoclassical prediction decreases with \bar{n}_e , contrary to the experimental data.
- FIG.2 Energy confinement time vs line-averaged density for Alcator C. Solid points represent data obtained with gas fueling. Open circles were obtained using frozen deuterium pellet injection. The solid curve is not a fit to the data but the result of a simulation with neo-Alcator electron transport and $1 \times$ neoclassical ion conduction.
- FIG.3 Ratio of observed ion thermal diffusivity to the theoretical value of Hinton and Hazletine [20], plotted as a function of plasma current and safety factor.
- FIG.4 Lawson confinement parameter $n_0 \tau_E$ for the data of Fig.2.
- FIG.5 Ratio of ion thermal diffusivity to the (Chang-Hinton) neoclassical prediction as a function of time during a pellet injection shot. The pellet is injected at 308 msec. Error bars represent the limits of code runs with input parameters varied over the range of experimental uncertainty.
- FIG.6 Confinement data from a number of ohmically heated tokamaks plotted against the neo-Alcator regression parameter. The fit was done for the devices in the legend at the upper left. Points from TFTR and JET agree well with the extrapolated line.
- FIG.7 Normalized chordal brightnesses of sodium- (1394 Å), beryllium- (303 Å), helium- (6.65 Å) and hydrogen-like (6.18 Å) silicon as well as the central soft-x-ray diode signal for a typical series of injections. Dashed curves are predictions from the computer model with a diffusion coefficient of $2.6 \times 10^{-1} \text{ m}^2 \cdot \text{s}^{-1}$.
- FIG.8 Impurity confinement times as a function of q_L^{-1} for aluminum, silicon and titanium injections into hydrogen, deuterium and helium plasmas.
- FIG.9a Electron temperature versus density. $B = 9\text{T}$, $I_p = 400 \text{ kA}$, $\text{PRF} = 0.85\text{MW}$, D_{plasma} .
- 9b Bulk ion temperature versus time. $\bar{n}_e = 1.4 \times 10^{20} \text{ cm}^{-3}$, $B = 9\text{T}$, $I_p = 400\text{kA}$.
- FIG.10 Current drive efficiency: a) $\bar{n}_e I$ versus P , and b) I/P versus \bar{n}_e . H_2 gas, flat-top plasma current without inductive drive.

FIG.11a ΔI versus waveguide phasing, $\Delta\phi$ in Versator II. $\Delta\phi > 0$ corresponds to wave propagation in the direction of ohmic electron drift.

11b Transmission coefficient T versus $\Delta\phi$.

11c ΔI versus \bar{n}_e , showing the density limit at $\bar{n}_e = 6 \times 10^{18} \text{ m}^{-3}$.

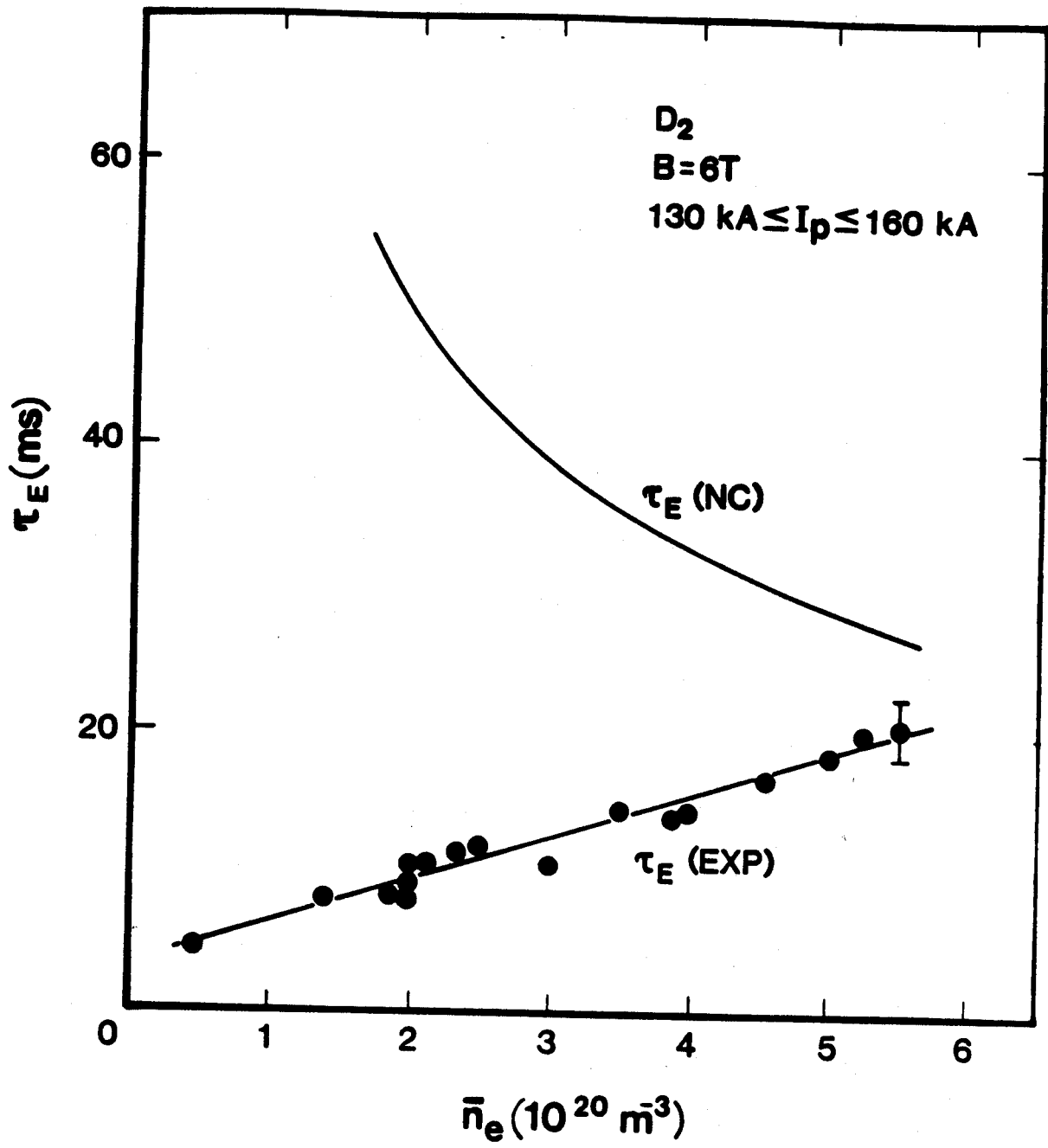


FIGURE 1

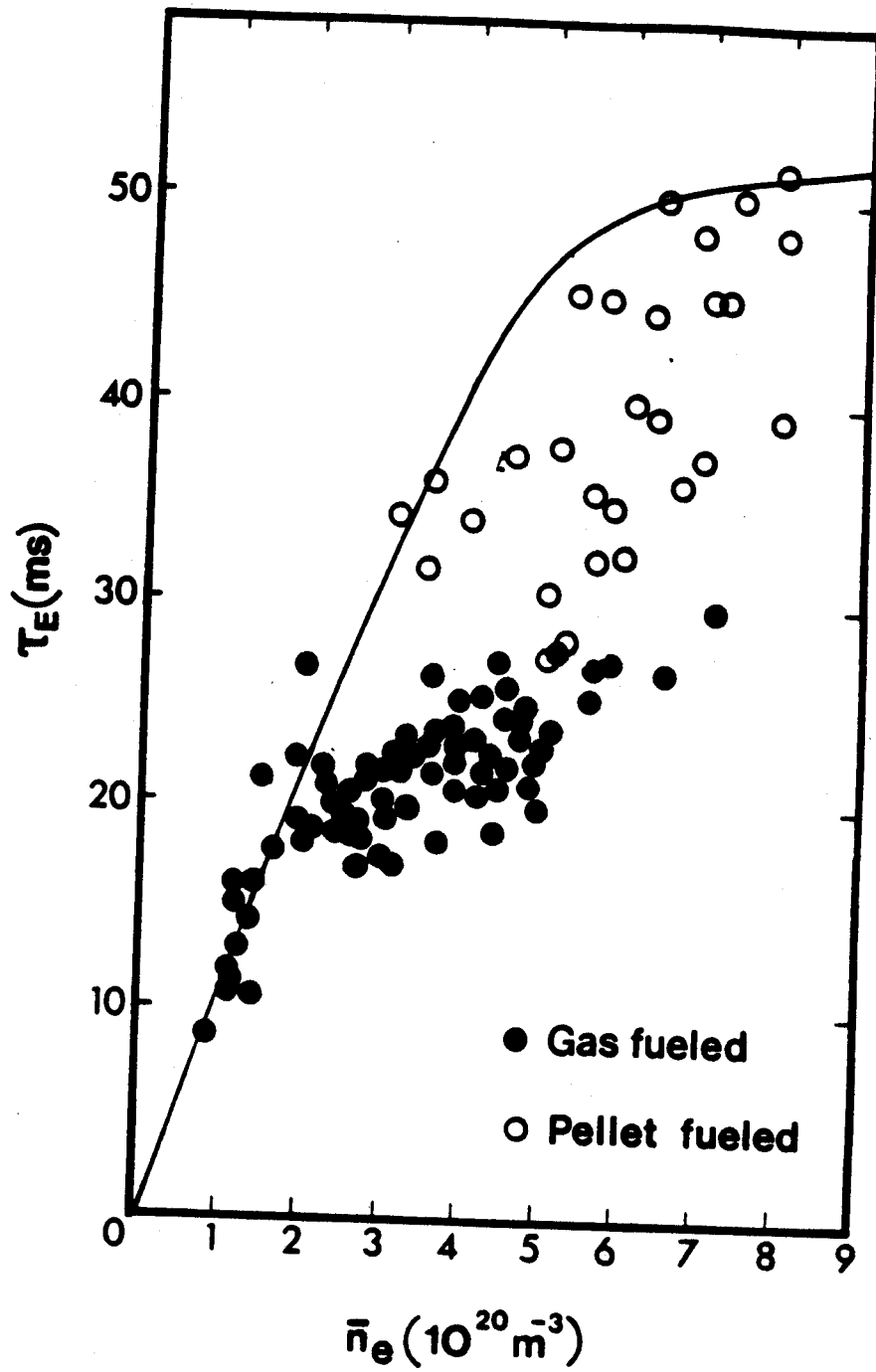


FIGURE 2

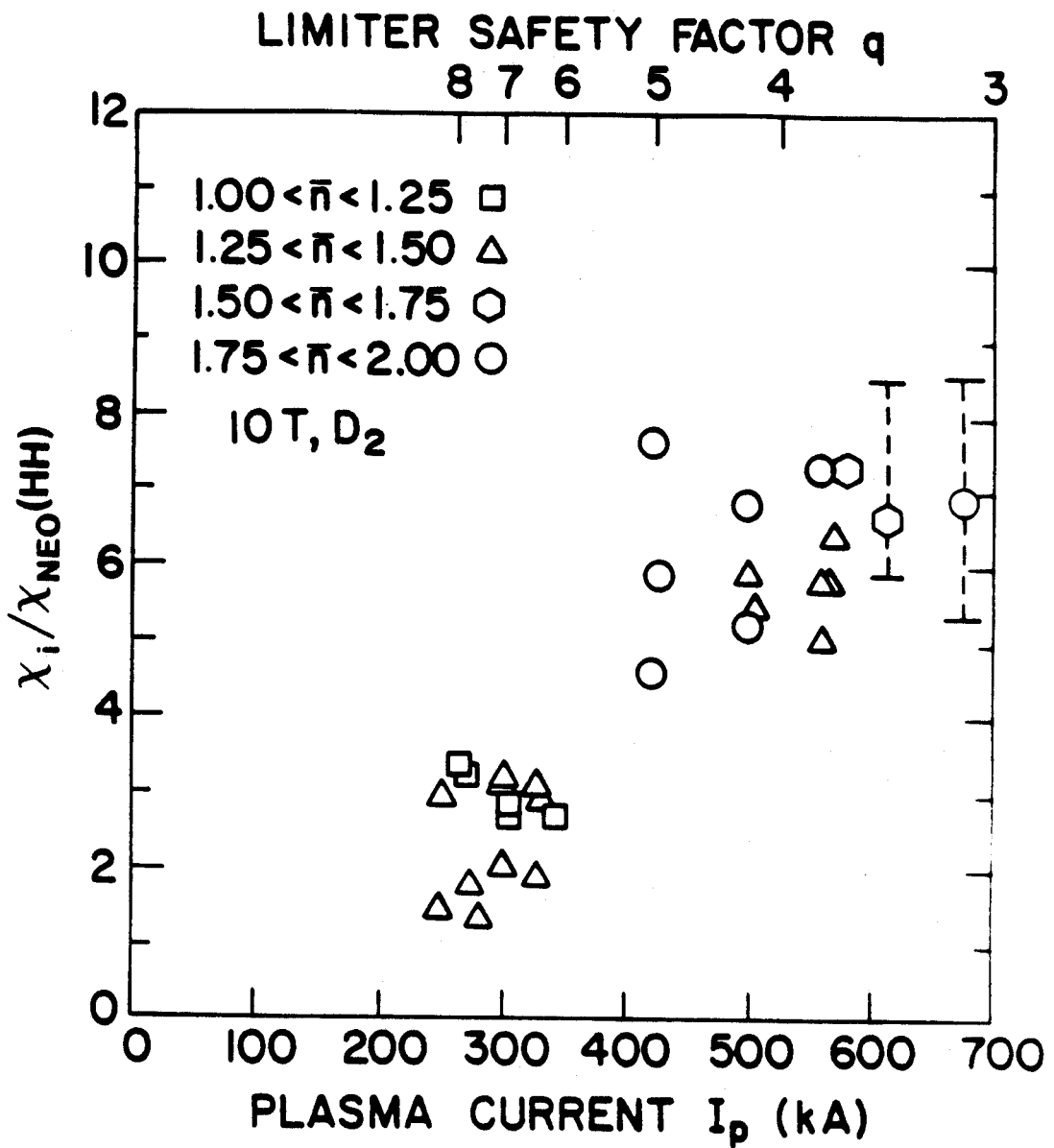


FIGURE 3

Confinement Parameter

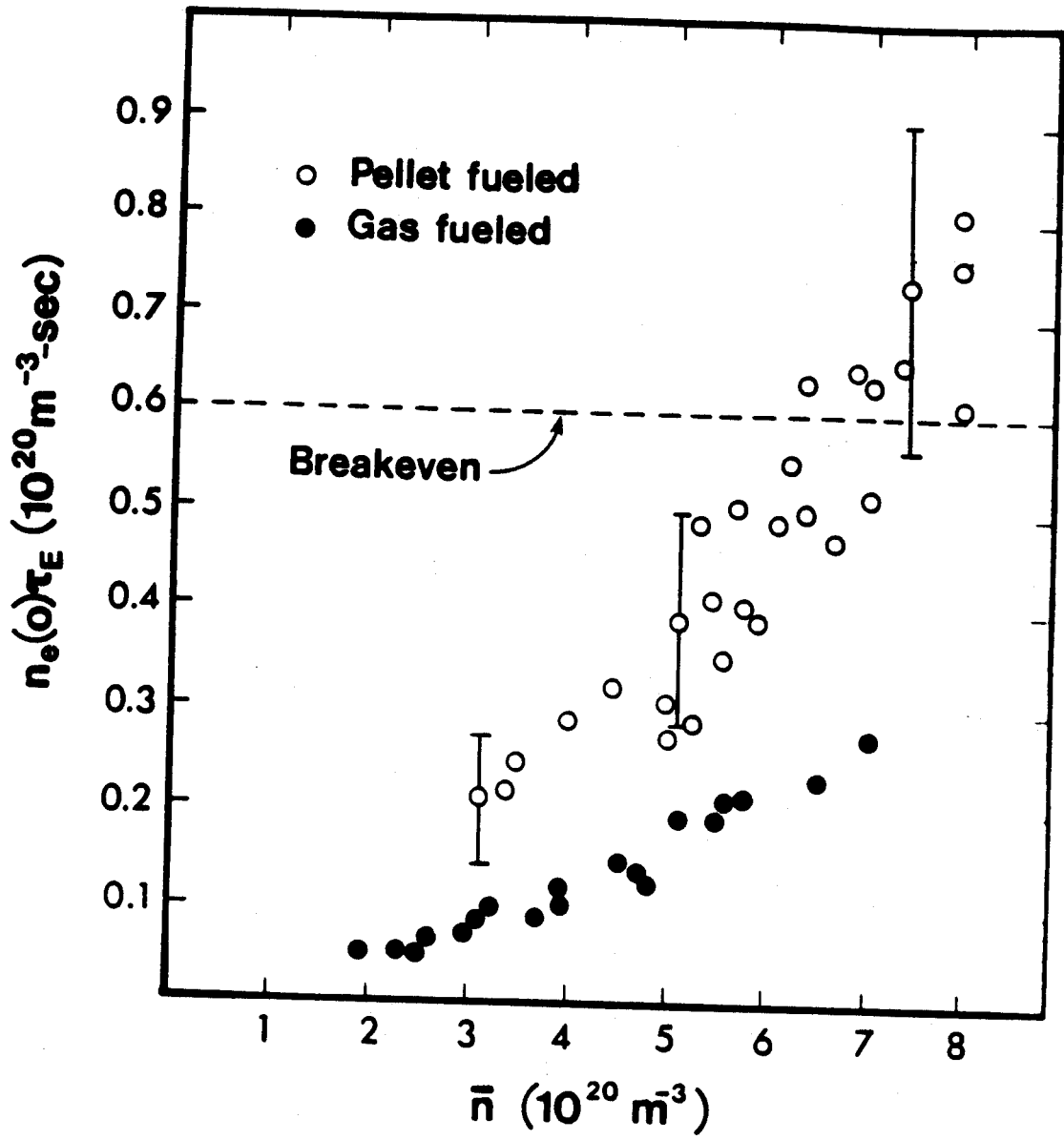


FIGURE 4

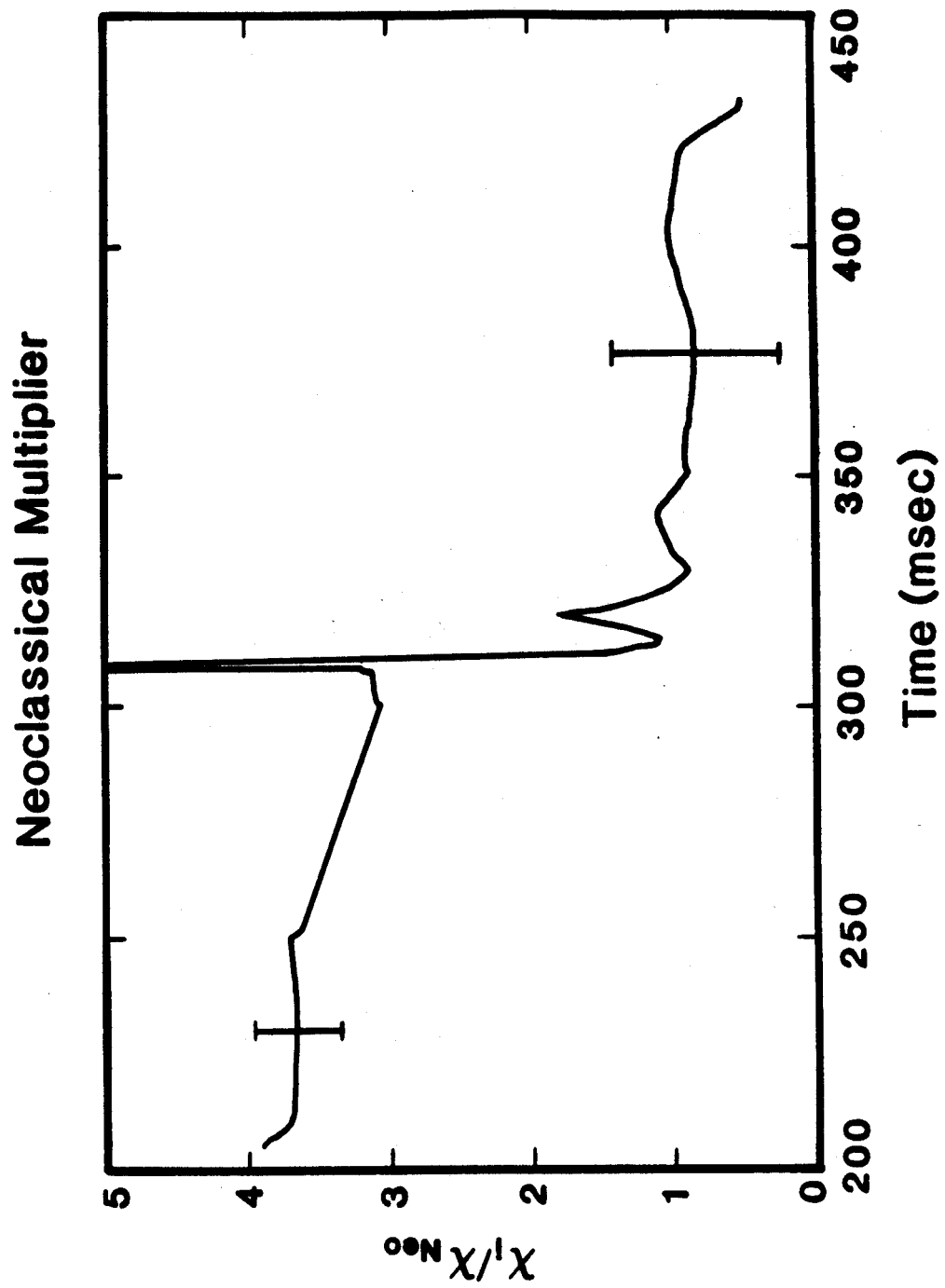


FIGURE 5

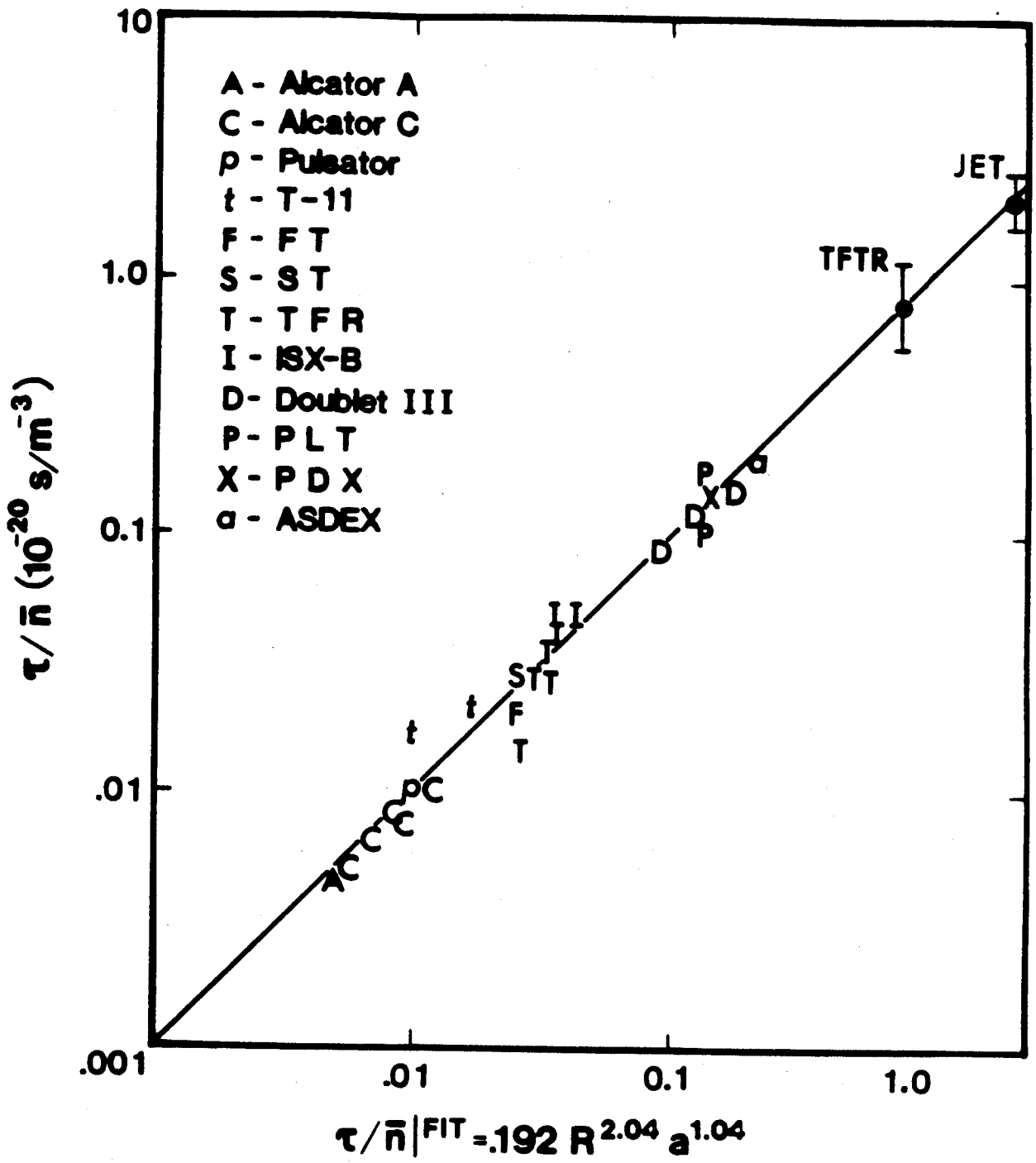
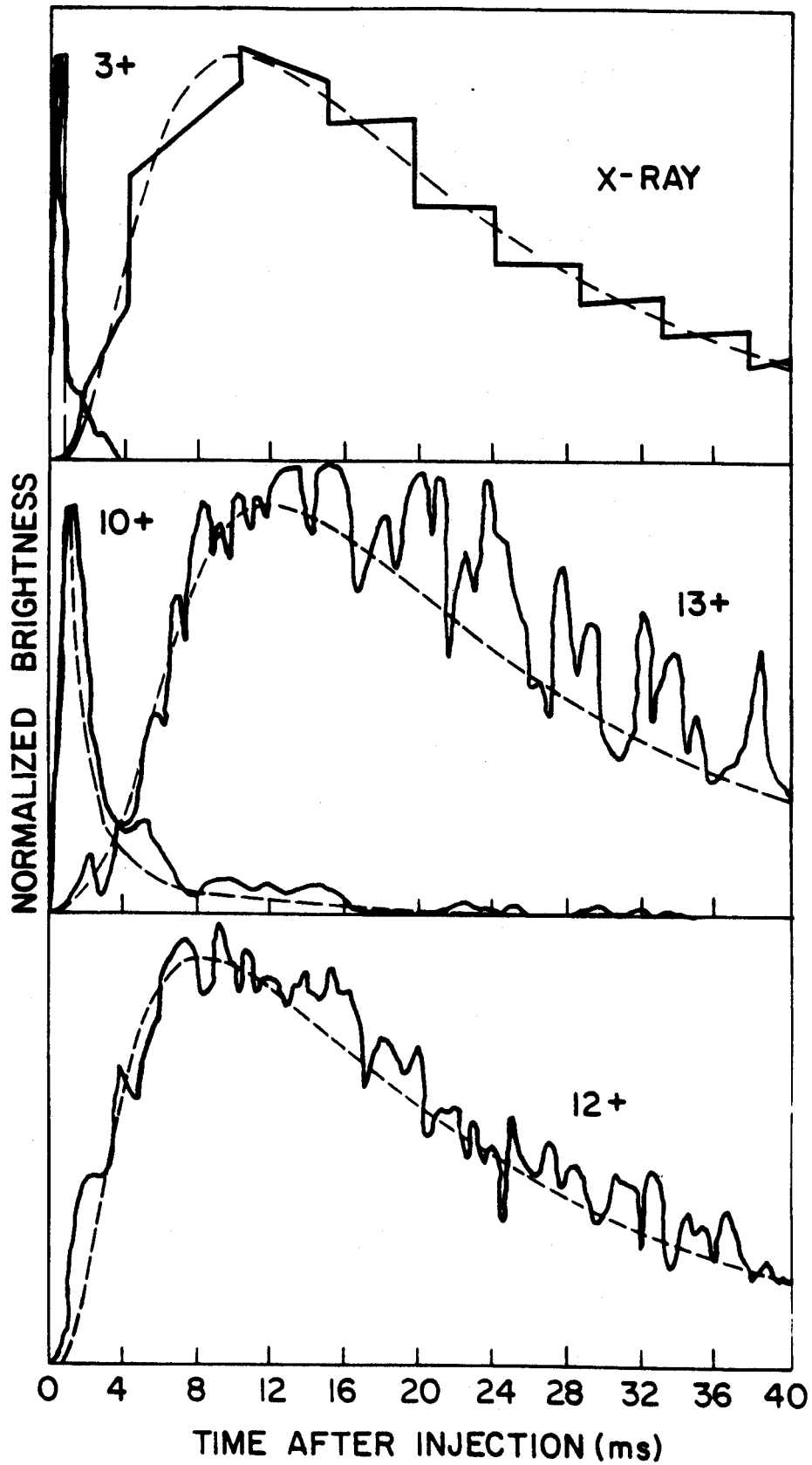


FIGURE 6



PFC-7092

FIGURE 7

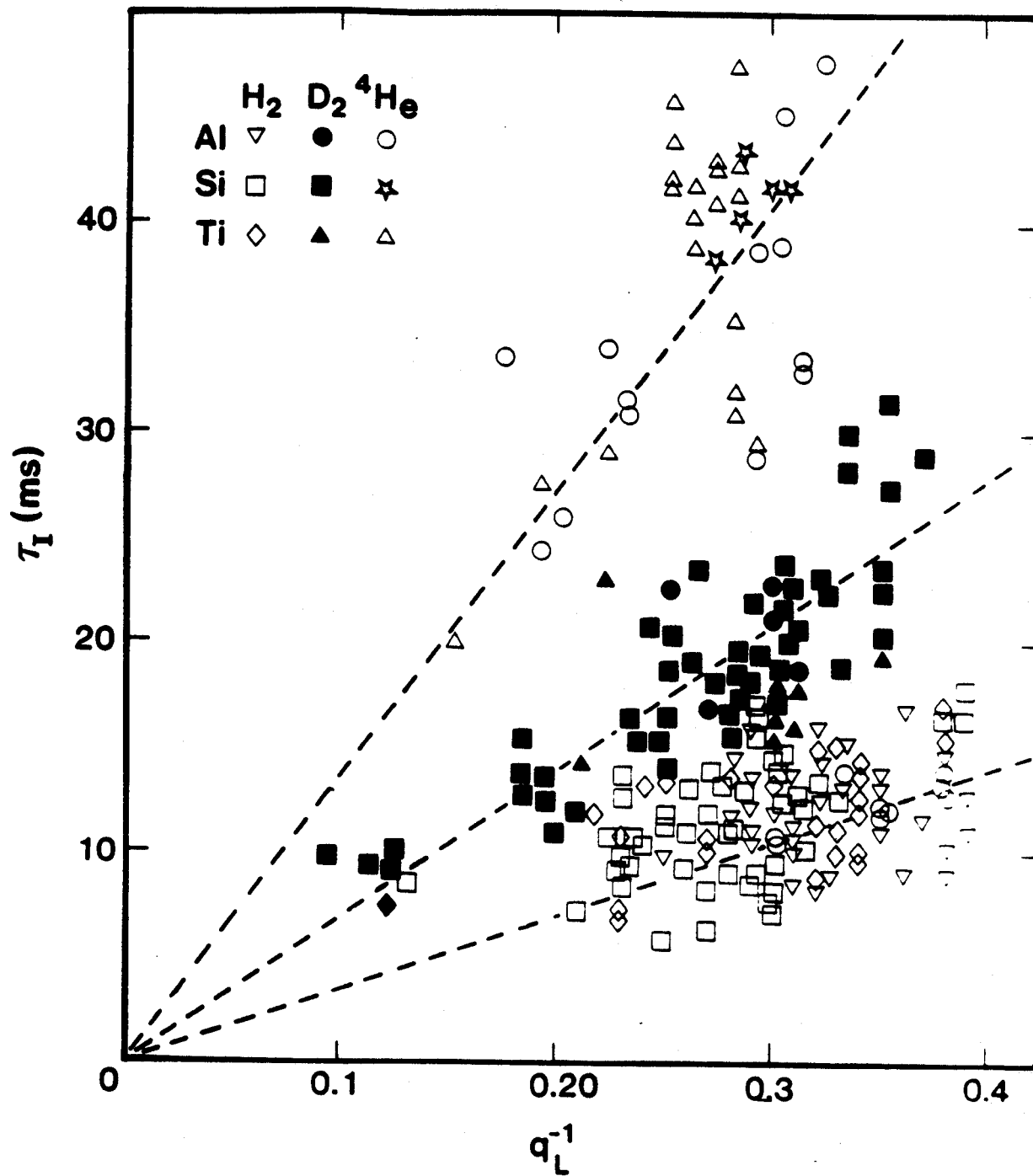


FIGURE 8

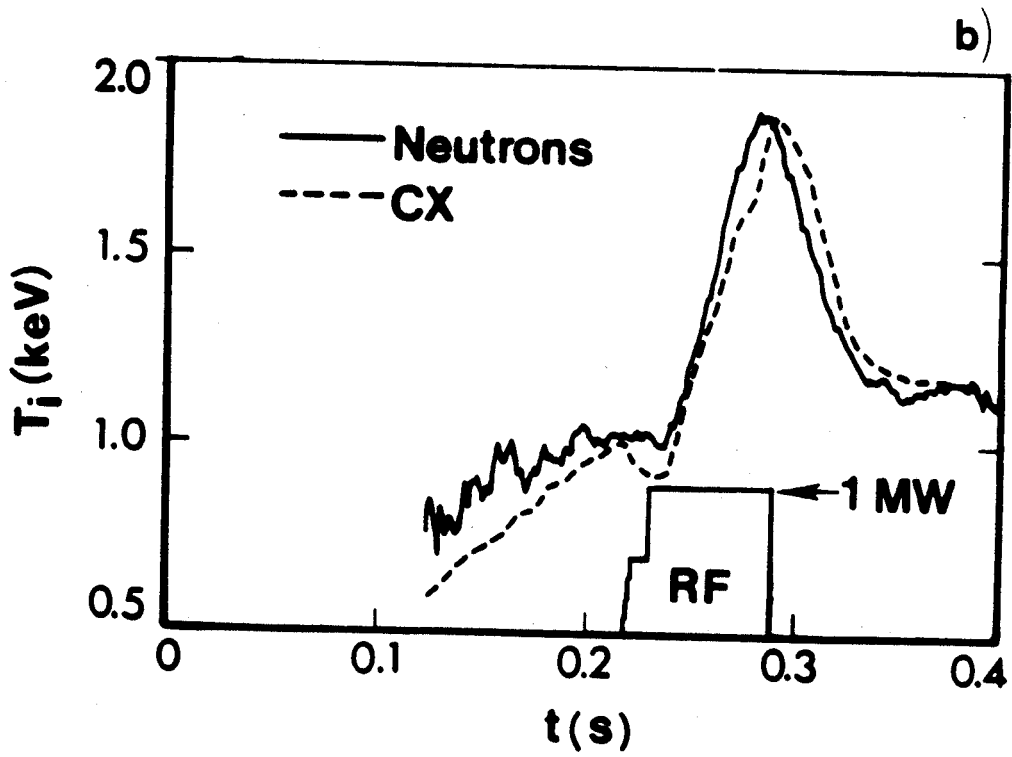
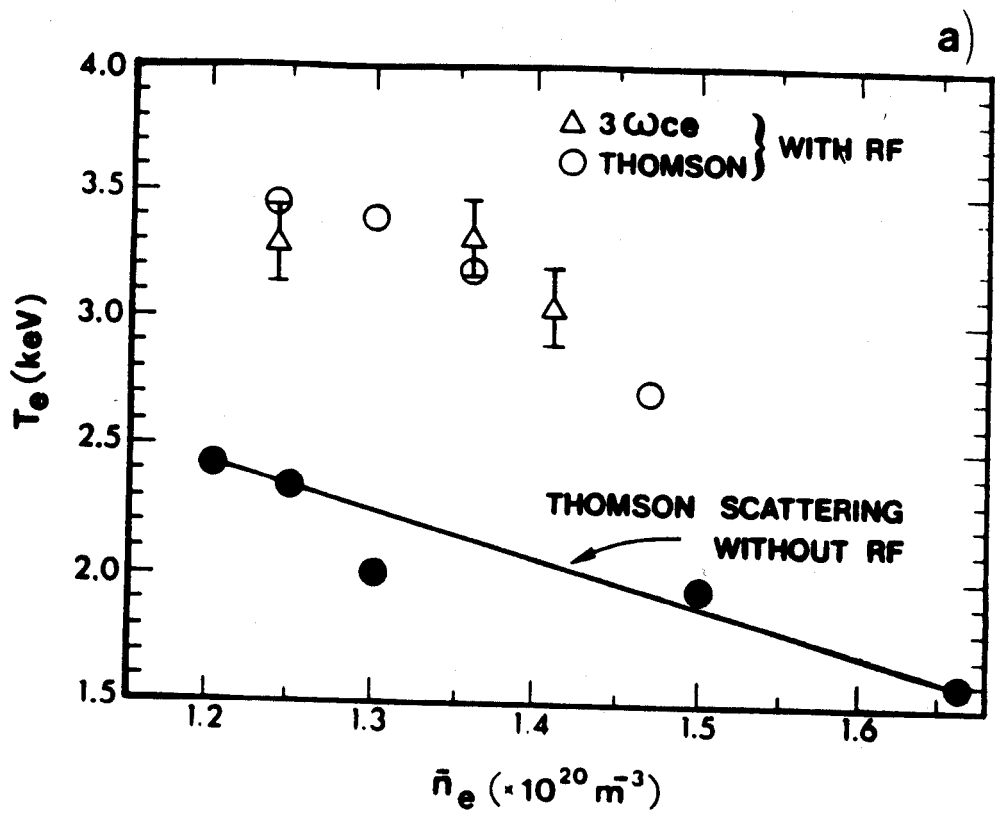


FIGURE 9

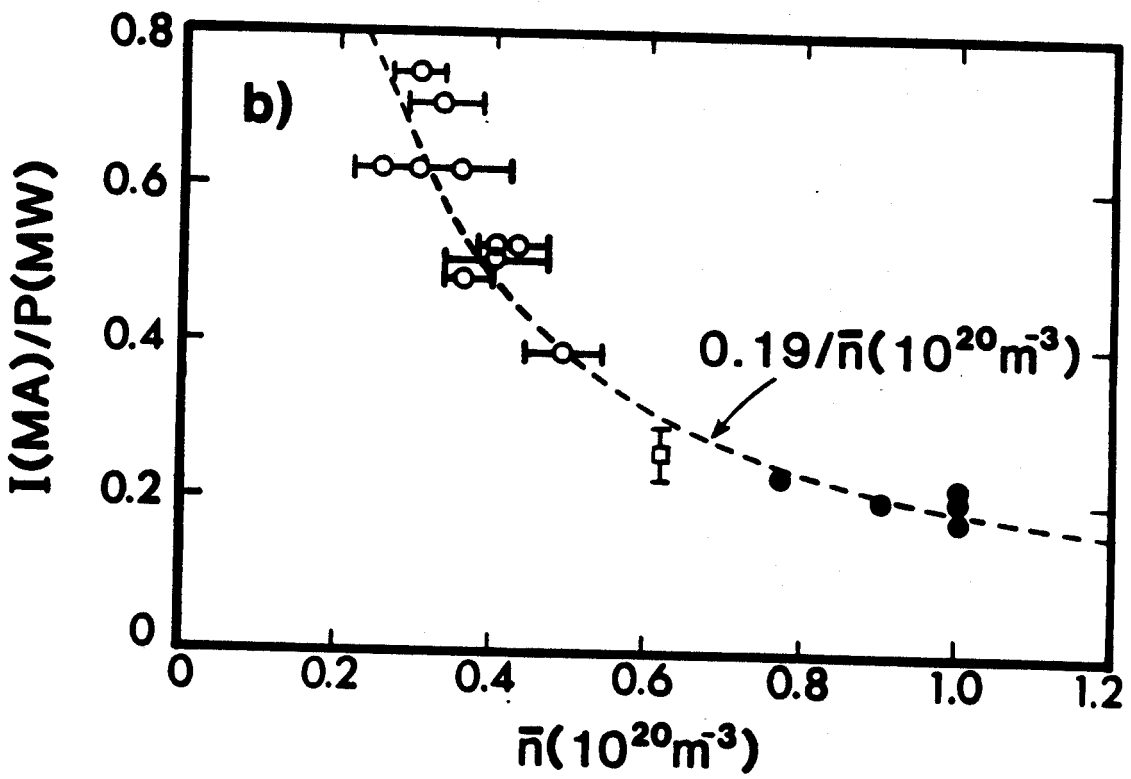
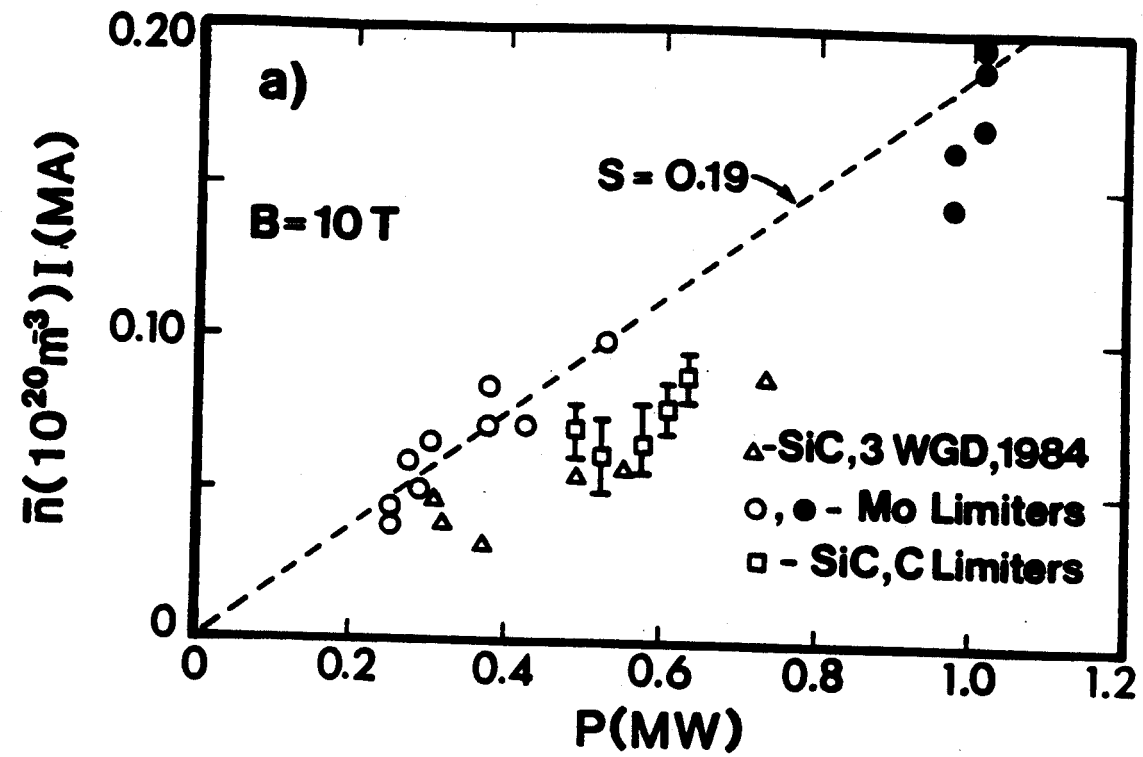


FIGURE 10

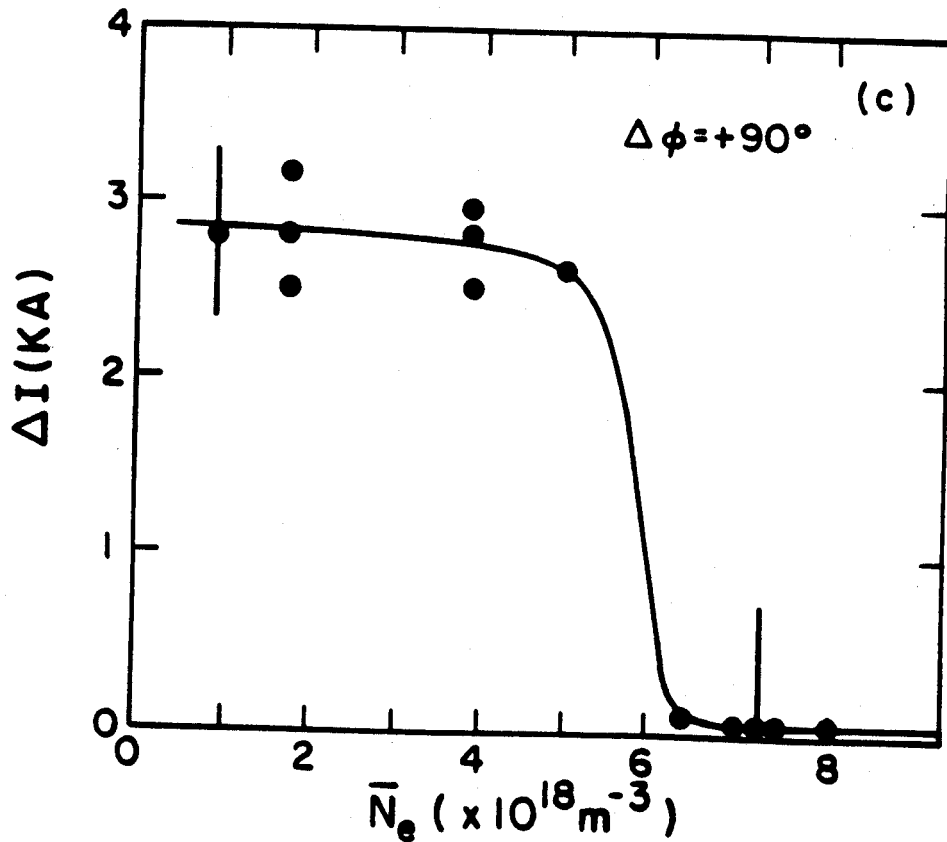
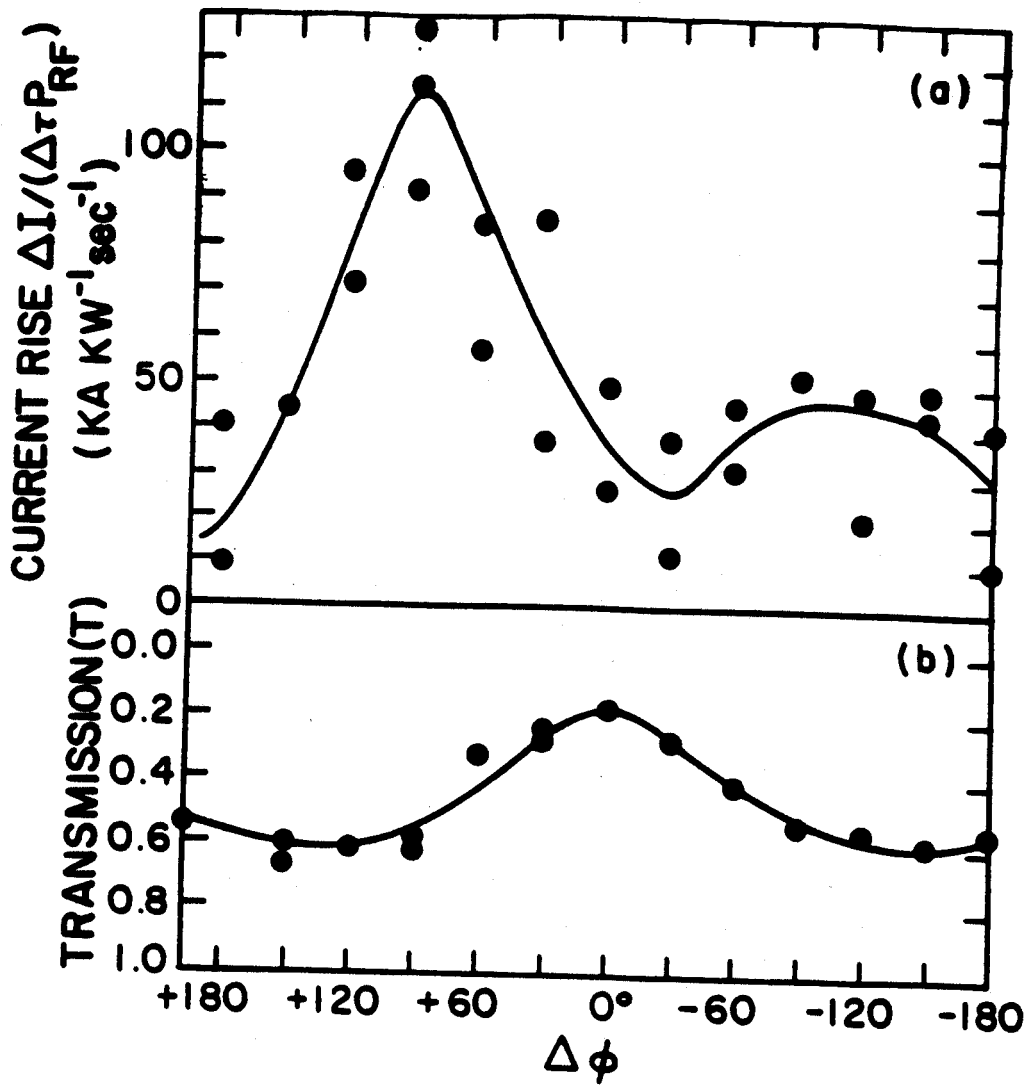


FIGURE 11